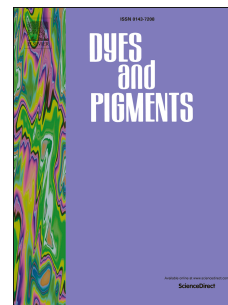


Journal Pre-proof

Naphthodipyrrolopyrrole-based Aza-BODIPY dye for N-type organic field-effect transistors

Chuanqi Miao, Dongxu Liang, Liang Gu, Changlin Li, Maning Liu, Jianhui Li, Paola Vivo, Haichang Zhang



PII: S0143-7208(22)00777-X

DOI: <https://doi.org/10.1016/j.dyepig.2022.110855>

Reference: DYPI 110855

To appear in: *Dyes and Pigments*

Received Date: 3 August 2022

Revised Date: 10 October 2022

Accepted Date: 12 October 2022

Please cite this article as: Miao C, Liang D, Gu L, Li C, Liu M, Li J, Vivo P, Zhang H, Naphthodipyrrolopyrrole-based Aza-BODIPY dye for N-type organic field-effect transistors, *Dyes and Pigments* (2022), doi: <https://doi.org/10.1016/j.dyepig.2022.110855>.

This is a PDF file of an article that has undergone enhancements after acceptance, such as the addition of a cover page and metadata, and formatting for readability, but it is not yet the definitive version of record. This version will undergo additional copyediting, typesetting and review before it is published in its final form, but we are providing this version to give early visibility of the article. Please note that, during the production process, errors may be discovered which could affect the content, and all legal disclaimers that apply to the journal pertain.

© 2022 Published by Elsevier Ltd.

Author Contribution Statement:

Chuanqi Miao: Investigation, formal analysis, data curation, writing- original draft preparation.

Dongxu Liang: Data curation, formal analysis.

Liang Gu: Data curation, formal analysis.

Changlin Li: Data curation, formal analysis.

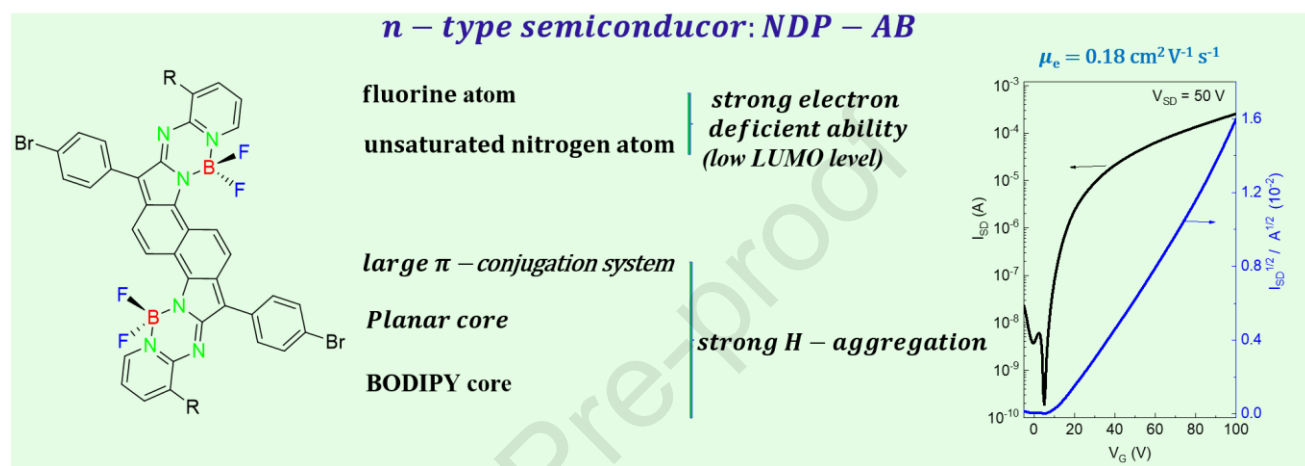
Maning Liu: Funding acquisition, writing- reviewing and editing.

Jianhui Li: Data curation, formal analysis.

Paola Vivo: Funding acquisition, writing- reviewing and editing.

Haichang Zhang: Supervision, writing- reviewing and editing, project administration, funding acquisition.

Graphic Abstract



Naphthodipyrrolopyrrole-based Aza-BODIPY Dye for N-type Organic Field-Effect Transistors

Chuanqi Miao, Dongxu Liang, Liang Gu, Changlin Li, Maning Liu, Jianhui Li, Paola Vivo, Haichang Zhang*

^aKey Laboratory of Rubber-Plastics of Ministry of Education/Shandong Province (QUST), School of Polymer Science and Engineering, Qingdao University of Science and Technology, 53-Zhengzhou Road, Qingdao 266042, P. R. China

^bHybrid Solar Cells, Faculty of Engineering and Natural Sciences, Tampere University, P.O. Box 541, Tampere FI-33014, Finland

*Corresponding author: E-mail: haichangzhang@hotmail.com

Abstract:

To date, n-type semiconductor designs are less investigated than their p-type counterparts, due to the fact that the charge transport mobility and the stability of the n-type materials are generally lower than those of the p-type ones. Well-defined n-type semiconductors often require low lowest unoccupied molecular orbital (LUMO) levels that facilitate the electron injection from the electrode into the semiconductors. Therefore, it is of significance to explore novel chromophores with strong electron-deficient properties, yet it is still challenging. Herein, a naphthodipyrrolopyrrole-based dimeric aza-boron dipyrromethene (Aza-BODIPY) dye (NDP-AB) is designed and synthesized. The optical studies indicate that NDP-AB presents a blue spectral shift (111 nm) in solution phase compared to the thin film state, while exhibiting a photoluminescence emission quenching. The NDP-AB semiconductor demonstrates strong acceptor properties with a low LUMO energy level of only -4.25 eV, owing to the multi-fluorine atoms, unsaturated nitrogen atoms, as well as the amide functional groups. Moreover, the large conjugation system, highly planar core, along with the large transition dipole on the line that links 2-position with 6-position of the BODIPY core, result in NDP-AB with a strong H-aggregation. As a consequence, the NDP-AB-based semiconductors show a good n-type behavior with an average electron mobility of $0.16 \text{ cm}^2 \text{ V}^{-1} \text{ s}^{-1}$. Our work, proposes a strong electron-deficient chromophore that is a promising candidate as building block of organic field-effect transistors. Our design strategy paves the way for the identification of more n-type semiconductor materials with high-performance.

1. Introduction

Over the last few years, π -conjugated semiconducting materials for organic field-effect transistors (OFETs) have attracted considerable attention due to their chemical structure tunability, low-cost mechanical flexibility, and large-area solution processability for electronic applications^[1-5]. To date, most of the reported conjugated materials are p-type semiconductors, while the research focusing on n-type or ambipolar conjugated materials greatly falls behind^[6-9]. This might be attributed to the fact that the n-type semiconductors are easy to be doped and sensitive to ambient conditions (e.g., moisture and oxygen), which results in their poor stability and low charge transport mobility compared to the p-type counterparts^[10-12]. Developing high-performance n-type or ambipolar semiconductor materials with high charge transport mobility and good stability is always very desired though challenging.

A good n-type conjugated material should feature not only low lowest unoccupied molecular orbital (LUMO) levels, but also high inter- and intra-charge transport mobilities^[13-16]. The low LUMO energy levels (typically below -4.0 eV) facilitate the electron injection from the electrode into the semiconductor layers, leading to the n-type or ambipolar properties^[17-20] for the conjugated materials. Materials with low LUMO values typically contain chromophores with strong electron-deficient properties^[21-22]. However, electron-deficient semiconductors are relatively less explored due to

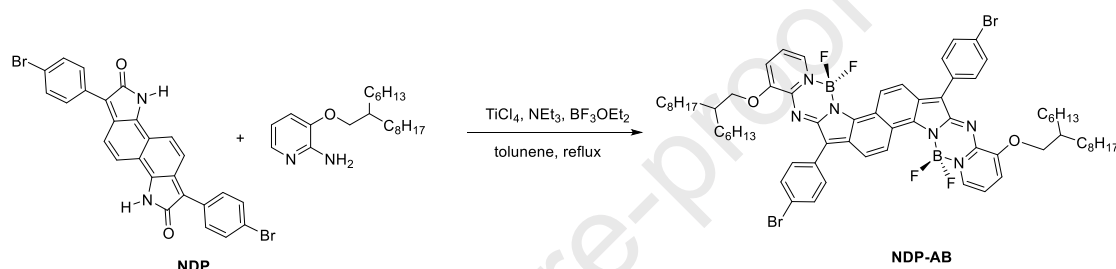
their tedious syntheses. Tremendous efforts have been made to explore the acceptor units with new structures for diverse applications [23-25]. Most of the reported chromophores with good properties contain the amide groups such as diketopyrrolopyrrole (DPP), benzodipyrrolidone (BDP), indigo, naphthodipyrrolidone (NDP) and their derivatives (see Figure S1 in the Supporting Information, SI) [26-32]. Recently, an NDP-based chromophore has attracted our attention. The chemical structure of NDP is similar to those of DPP and BDP except that the DPP and BDP cores are bi- and tricyclic, whereas the NDP is tetracyclic (Figure S1). NDP was firstly developed by B. Tiede's group in 2014^[33]. Later on, Zhu's group synthesized NDP-based polymers in OFETs, which exhibit stable n-type properties^[34]. To the best of our knowledge, almost all the reported NDP-based chromophores present n-type or ambipolar properties, which are suitable building blocks for the fabrication of n-type or ambipolar semiconductors^[34-36]. However, further optimization of NDP structures is still desirable for the development of n-type or ambipolar semiconductor materials.

In the semiconductor layer, the charge carriers need to be efficiently transferred between individual molecules in order to be transported from one electrode to the other. Therefore, the molecular packing mode is critical for realizing efficient charge transport^[37]. Compared to the J-aggregation, the H-aggregation is more favorable for the charge transport, since it is a face-to-face parallel aggregation that results in a good π - π aggregation as well as π - π overlap, in turn leading to materials with improved intermolecular charge transport mobility^[38-42]. However, it is generally difficult to design and synthesize materials with H-aggregation. Tokoro et al. reported that 4,4-difluoro-4-bora-3a,4a-diaza-s-indacene (BODIPY) dyes can stack geometrically in the form of H-dimers due to a large transition dipole on the line that links 2-position with 6-position of the BODIPY core^[43-44]. In the H-dimer, two BODIPY planes stack with almost both parallel $S_0 \rightarrow S_1$ transition dipoles and antiparallel electric dipole moments. This research has inspired us to adopt BODIPY building blocks to modify the NDP chromophore with the design and synthesis of the first NDP-based Aza-BODIPY (NDP-AB) n-type semiconductor proposed in this work. NDP-AB exhibits the H-aggregation and, in addition, compared to NDP, it presents large and effective π -conjugation system, which is beneficial for the charge transport within the single molecules. Besides, the NDP-AB contains multi-fluorine (F) atoms and unsaturated nitrogen atoms, which can improve the electron-deficient property, thus deepening the LUMO levels.^[45-48] Based on these merits, the NDP-AB could be a promising material for n-type or ambipolar chromophore for the application of OFETs.

The NDP-AB are theoretically and experimentally investigated by using the quantum chemical calculations (B3LYP/6-31G*), spectroscopic methods (e.g., nuclear magnetic resonance (NMR) and UV/visible spectrometer), cyclic voltammetry, and X-ray diffraction (XRD). In addition, high-performance OFETs are fabricated by employing the NDP-AB small molecule as the n-type semiconductor layer. The NDP-AB-based chromophore shows outstanding electron-deficient property with a relatively low LUMO level of around -4.25 eV with broad optical absorption (between 550 and 850 nm). In addition, the NDP-AB present a strong H-aggregation. The as-fabricated OFETs exhibit n-type behavior with an electron mobility (μ_e) up to 0.18 cm² V⁻¹ s⁻¹.

2. Results and discussion

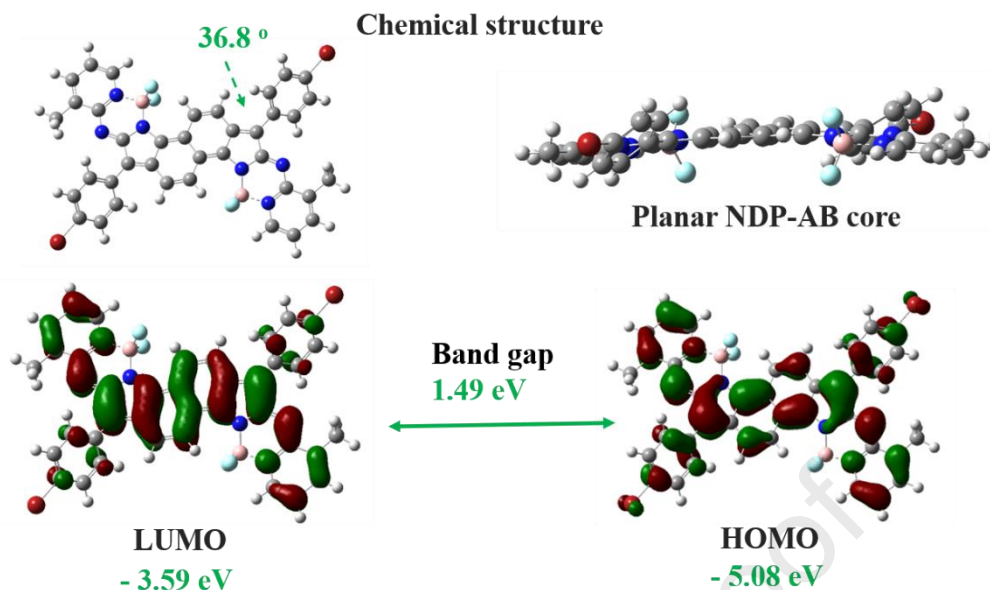
The NDP-AB chromophore was synthesized by utilizing the Schiff-base reaction of NDP and heteroaromatic amines with a yield of 39 % (Scheme 1). The as-synthesized NDP-AB was characterized by NMR, elemental analysis, and mass spectroscopy, confirming the successful synthesis of the NDP-AB chromophore. The NMR spectra of the compounds exhibit all the expected resonance peaks (Figures S2 – S3). The proton signal on the alky chain lies between 0.90 and 4.06 ppm, while the observed signals between 7.16 and 8.34 ppm are ascribed to the protons from the aromatic ring units. NDP-AB presents good solubility in most common organic solvents such as chloroform, toluene, and acetone, owing to the alky side chains.



Scheme 1. Synthetic route leading to NDP-AB.

2.1 Computation study

In order to investigate the molecular structure of NDP-AB, computational calculations were conducted via density-functional theory (DFT) at the B3LYP/6-31 (d,p) level by using a simplified NDP-AB structure with a methyl group substituted unit. The optimized structures reveal that the core of NDP-AB, along the aza-BODIPY-NDP axis, is in the same plane (Figure 1). The dihedral angle between the phenyl ring and the NDP-AB core is around 36.8°. The highly coplanar backbone structure of NDP-AB molecules could facilitate the efficient intramolecular charge delocalization within NDP-AB molecules, which is also beneficial for achieving close intermolecular stackings in the solid state. The electrons at the highest occupied molecular orbital (HOMO) level of NDP-AB are well-distributed along with the whole molecule, while the electron cloud density distribution of the LUMO level is mainly localized at the NDP-AB core. Once the molecule is excited, the electrons transfer from the whole molecule to the NDP-AB core will occur. The calculated HOMO and LUMO levels of NDP-AB are -5.08 eV and -3.59 eV, respectively, and the band gap is estimated as 1.49 eV.



14

Figure 1. Structures and molecular orbital surfaces of HOMO and LUMO of NDP-AB obtained at the B3LYP/6-31 (d,p) level.

2.2 Thermal properties

The thermal properties of NDP-AB were characterized by thermogravimetric analysis (TGA) and differential scanning chromatography (DSC). As shown in Figure S6, the TGA spectra demonstrate that there is no weight loss before 270 °C, and the 5% weight loss occurs at 330 °C for NDP-AB. Most of the B←N incorporated materials show the low stability. However, the DSC curves of NDP-AB exhibit no any exothermic peak observed during the heating cycle between 30 °C and 270 °C, indicating that the B←N bond is stable when incorporated in the NDP-AB core. The DSC traces of the NDP-AB present an exothermal transition that is located in the range between 50 °C and 100 °C during the heating process, ascribed to the glass transition temperature (T_g).^[49-50] Correspondingly, the endothermic transition was observed at ~123 °C during the cooling process, stemming from the formation of some ordered structures for the alkyl side chain attached NDP-AB core when the temperature was decreased. The DSC and TGA curves reveal that NDP-AB possesses a good thermal stability.

2.3 Optical properties (H-aggregation)

To investigate the molecular aggregation in the solid state, the absorption spectra of the solution and thin film were measured. The corresponding optical data are summarized in Table S1 in the SI. The NDP-AB solution in tetrahydrofuran (THF) turns

into a blue color with an absorption peak at 770 nm accompanied by a shoulder at 707 nm, while the NDP-AB-based thin film exhibits a cyan color with an exciton peak at 659 nm (Figure S2 and Figure 2c). Most of the conjugated materials in their solution phase likely form a single-molecular state, with the absorption maximum generally exhibiting a red-shift^[51-53] in the solid state compared to the solution case. On contrary, NDP-AB shows an opposite trend with the blue-shifted absorption maximum in solid state by almost 111 nm compared to that in solution, while the absorption onset is red-shift by 230 nm (from 820 nm in solution to 1004 nm in film state). Based on the absorption onset, the optical band gap of NDP-AB is calculated to be 1.24 eV. The large spectral blue-shift for the absorption maximum and the red-shift for the absorption onset indicate that NDP-AB thin film possesses a strong aggregation and close packing, which are advantageous for realizing the efficient charge transport between the neighboring molecules. In addition, the optical blue-shift for the absorption maximum hints that the NDP-AB film could feature a H-aggregation, whose formation benefits from the large conjugation system, good planar core-structure, and large transition dipole on the line that links 2-position with 6-position of the BODIPY core^[54-56].

To further identify the NDP-AB film molecular packing with H-aggregation, the absorption and photoluminescence (PL) spectra of NDP-AB were carried out for the mixture solutions of THF and water (volume: volume, v:v (THF:H₂O) = 10:0; 8:2; 6:4; 4:6; 2:8; 0:10). As shown in Figure 2a, NDP-AB exhibits a strong absorption peak at 770 nm that is assigned to the S₀→S₁ transition of the monomeric NDP-AB (Figure 2a). In the solvent of THF-containing water, an increase in the water ratio induces a gradual decrease in the molar absorption coefficient at the absorption maxima until the THF:H₂O ratio is 6:4. The absorption spectra of NDP-AB present a new peak at 659 nm when the ratio of THF:H₂O is below 4:6. At this stage, the solution turns from blue to almost transparent with a cyan color (Figure 2c). The new peak appearance is ascribed to the formation of H-dimers of NDP-AB. When increasing the water content, the new peak intensity is enhanced with a signature of more H-dimers formation. For H-aggregation, the H-dimers are practically non-fluorescent with a blue-shifted absorption compared to their monomer case. As observed in Figure 2b, the fluorescence intensity of NDP-AB is decreased with no change on the peak position along with the addition of water in the mixture. Particularly, there is a sharp decrease when the THF:H₂O ratio changes from 6:4 to 4:6 upon the fluorescence quenching (Figures 2b and 2c). This trend is also observed in the absorption spectra. The absorption and emission spectra of the NDP-AB film are similar to those in the pure water (Figure 2d). All these observations confirm that NDP-AB exhibits a H-aggregation behavior^[43,57-58]. Figure S7 shows that NDP-AB presents almost the identical absorption spectra in different solvents (THF vs. chloroform), as well as in different states (thin film vs. water solution) as observed above. This suggests that the NDP-AB film obtained by spin-coating the chloroform-based precursor indeed presents the H-aggregation. The as-formed H-aggregation could be beneficial for the NDP-AB core π - π overlap, as well as the charge transport between the neighboring molecules.

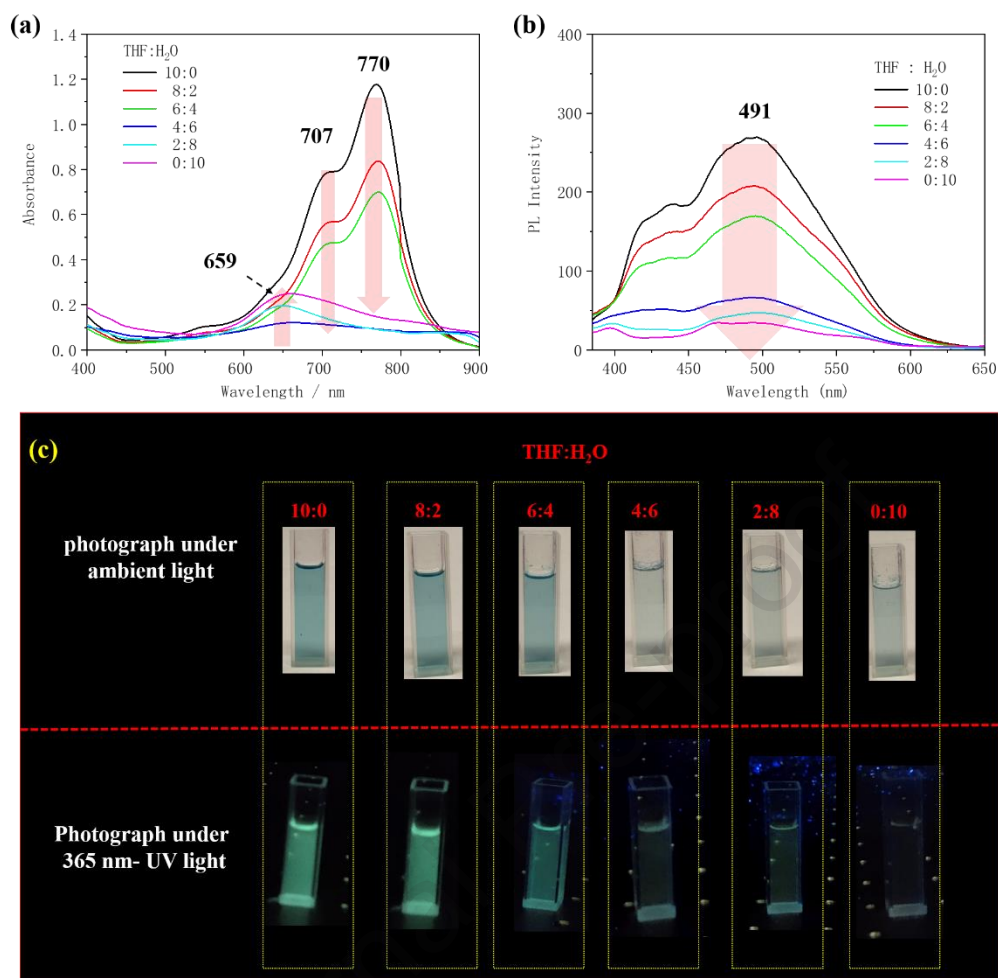


Figure 2. UV/vis absorption spectra (a) and emission spectra (b) of NDP-AB in THF-containing water with different ratios. (c) Photographs of NDP-AB in THF-containing water with different ratios under ambient light (top) and 365 nm UV light (bottom). The volume ratios of THF:H₂O is 10:0, 8:2, 6:4, 4:6, 2:8, 0:10.

2.4 Electrochemical properties

The electrochemical properties of NDP-AB were investigated by cyclic voltammetry (CV). The experimental details are described in the SI. Based on the onset reduction and oxidation potentials, the LUMO/HOMO energy levels of the material were estimated. Figure 3a shows that NDP-AB has the reversible cathodic and quasi-reversible anodic waves. The onset oxidation and reduction occur at 0.78 V and -0.55 V, from which the HOMO and LUMO energy levels were calculated as -5.58 eV and -4.25 eV, respectively. The extraordinarily low LUMO energy levels of NDP-AB are possibly caused by the strong electron-deficient properties of the molecules, originating from the amide group, fluorine atoms as well as the unsaturated nitrogen atoms in the NDP-AB core, since the acceptor ability mainly contributes to the alignment of LUMO energy levels.

Due to the low LUMO energy level of NDP-AB, the electron injection speed from

the electrode to the semiconductors could be optimized, leading to n-type or ambipolar properties for NDP-AB. In addition, the LUMO level is still higher than the reduction threshold of the weak nucleophiles (-4.6 eV), which allows NDP-AB to be a promising semiconductor with high environmental stability. From the onset oxidation and reduction peaks, the electrochemical band gap was calculated to be 1.33 eV. The HOMO/LUMO levels and the band gap obtained through the CV measurements are slightly different from the computationally calculated. This could be due to the fact that the DFT results were calculated based on the single molecules of the NDP-AB, while the CV measurements were carried out for the NDP-AB thin films with strong intermolecular interactions, such as the H-aggregation.

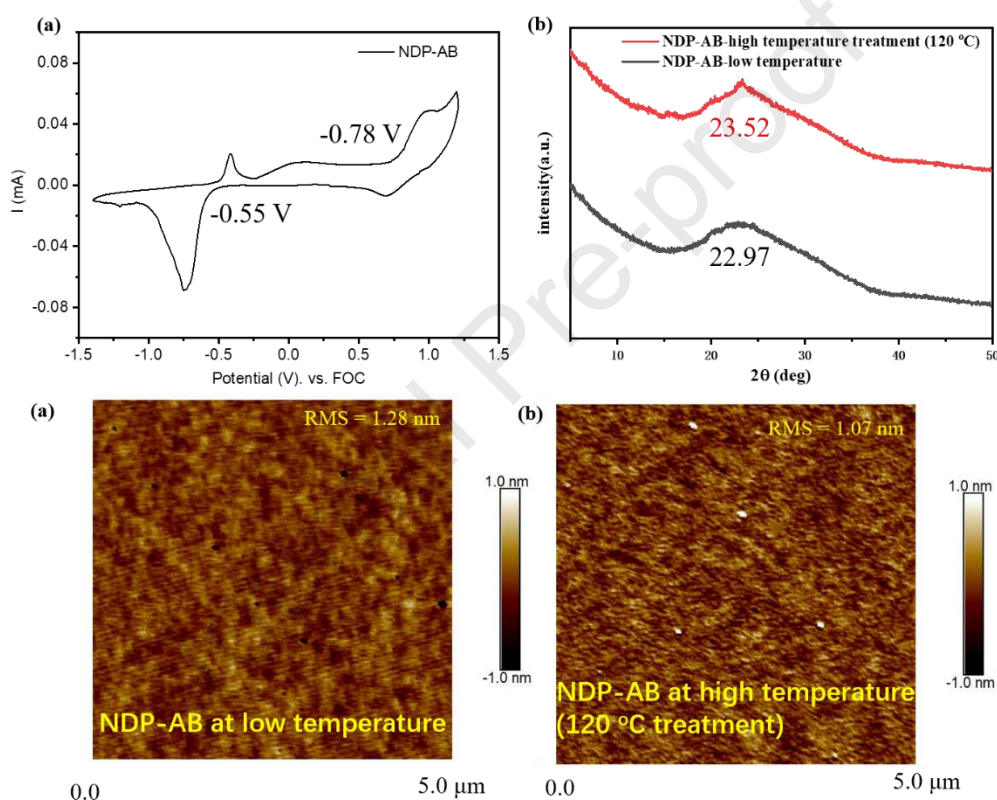


Figure 3. (a) Cyclic voltammograms of NDP-AB (spin-coated thin film on the ITO glass). Electrolyte: 0.1 M tetrabutylammonium hexafluorophosphate in acetonitrile. Potential calculated versus ferrocene. Scan rate: 100 mV s⁻¹. Temperature: room temperature. (b) Transmission XRD patterns of the NDP-AB films prepared via spin-coating before (low temperature, room temperature) and after thermal annealing at 120 °C (high temperature), respectively. (c,d) AFM images of the NDP-AB film before (c, low temperature) and after thermal annealing at 120 °C (d, high temperature, size of 5 × 5 μm).

2.5 Thin film

For small molecule-based OFETs, the charge carriers need to be efficiently

transferred between the individual molecules. Thus, the small molecules packing as well as the thin film morphology can significantly influence the performance of the OFETs. The thin film properties were probed by conducting the X-ray diffraction (XRD) measurements for the NDP-AB film with and without the thermal annealing treatment. As shown in Figure 3b, the pristine NDP-AB film exhibits an intermolecular co-facial π - π stacking peak at 22.97° , corresponding to a d -spacing of 0.387 nm. After the thermal annealing treatment at 120°C , the XRD pattern of the film turns to be sharper than that of the pristine one. Moreover, the π - π stacking peak shifts to 23.52° with a slightly decreased d -spacing of 0.378 nm. These observations possibly confirm the formation of more ordered molecular packing for the NDP-AB molecules upon the thermal annealing.^[59-62] This phenomenon could be caused by the nature of NDP-AB molecules after glass state, which suppresses the strong intermolecular interaction, such as molecular crystallization and π - π interactions.^[50]

The morphology of the NDP-AB thin film was investigated by atomic force microscopy (AFM) and the images are shown in Figure 3c. The surface of the film is quite smooth with a root-mean-square (RMS) roughness of 1.28 nm, demonstrating a well-distributed and flat morphology, which can afford superior film-forming capabilities. However, A disordered state with inferior crystallinity is also observed for the NDP-AB film. Upon the thermal annealing at 120°C , the morphology of the film is almost identical with that of the pristine case, except for a few interconnected small-sized crystalline grains with a reduced RMS roughness of 1.07 nm observed, which might be caused by the glass state of NDP-AB annealed at 120°C .^[50]

2.6 OFETs

The charge transport properties of the NDP-AB were evaluated by fabricating the OFET devices with NDP-AB as the semiconductor layer in a bottom-gate and bottom-contact (BGBC) configuration, which is based on an n-type silicon wafer by using a 300 nm SiO_2 layer as the dielectric material. The devices with the chromophores were fabricated by directly spin-coating the NDP-AB precursor in chloroform onto the octadecyltrichlorosilane (OTS)-treated silicon wafer with pre-patterned gold source and drain electrodes. The as-prepared devices were characterized before and after thermal annealing treatment at 120°C under vacuum condition. The detailed fabrication and testing procedures are described in the SI. The properties of as-fabricated OFETs are summarized in Table S2. As shown in Figure 4, the NDP-AB presents n-type properties with an average electron transport mobility of $0.10\text{ cm}^2\text{ V}^{-1}\text{ s}^{-1}$ (highest μ_e of $0.11\text{ cm}^2\text{ V}^{-1}\text{ s}^{-1}$). This average value can be further improved up to $0.16\text{ cm}^2\text{ V}^{-1}\text{ s}^{-1}$ (highest μ_e of $0.18\text{ cm}^2\text{ V}^{-1}\text{ s}^{-1}$) upon the thermal annealing at 120°C . The high μ_e achieved by the n-type NDP-AB can be attributed to: (i) ultra-low LUMO energy level, which is favorable for the electron injection from the electrode to the NDP-AB layer; (ii) the strong electron-deficient behavior of NDP-AB that can stabilize the electron transport within the semiconductor layer; (iii) high planar NDP-AB core as well as large π -conjugation system that result in the fast and efficient electron transfer within the NDP-AB single molecules; (iv) strong H-aggregation-containing NDP-AB film with

enhanced π -orbital overlap, where the charge transport occurs. Thus, all these factors are also beneficial for the charge transport across the adjacent molecules. Furthermore, the improved electron transport mobility in terms of thermal annealing process is likely due to the formation of strengthened molecular packing in the thin film, which has been confirmed by previous XRD and AFM studies. The threshold voltage (V_{th}) of the NDP-AB-based OFET is around 12 V, and it drops to 9 V after the thermal annealing. The decreased V_{th} value is possibly ascribed to that the fact that traps and defects in the semiconductor layer can be eliminated or at least significantly reduced upon the thermal annealing treatment. The current ratio (I_{on}/I_{off}) is in the range $10^5\sim 10^6$. During the last several years, some other Aza-BODIPY small molecules and polymers have also been investigated, most of which exhibit the n-type or ambipolar behavior with very few cases that demonstrate a p-type behavior (Figure S8). Most of the small molecules show the n-type behavior with the electron transport mobility in the range of $10^{-5}\sim 10^{-2}$ $\text{cm}^2 \text{V}^{-1} \text{s}^{-1}$. In addition, the BDP- and DPP-based small molecules, whose chemical structures are similar to the NDP, present the charge transport mobility of $10^{-3}\sim 10^{-2}$ $\text{cm}^2 \text{V}^{-1} \text{s}^{-1}$.^[63-67] However, the NDP-AB in this work features a high electron transport mobility up to $0.18 \text{ cm}^2 \text{V}^{-1} \text{s}^{-1}$, possibly due to the large conjugation system as well as to the good planar structure.

Normally, n-type OFETs are easy to be doped and sensitive to the ambient conditions (e.g., moisture and oxygen). To investigate the NDP-AB-based OFETs' stability, the pristine and thermal treated devices were separately exposed to the ambient conditions and Ar-filled glove box for one week after the fabrication, and the charge transport mobilities were continuously monitored under vacuum. The charge transport mobility exhibited almost no change after one week storage in the Ar-filled glove box. However, after the five days of exposure to the ambient conditions, the charge carrier mobility can retain nearly 68% of its initial value in the case of NDP-AB, and then displayed almost no change till the end of one week storage. During the same period, the electron transport mobility of the annealed devices can in turn maintain nearly 80% of its initial value. The annealed devices obviously exhibit an improved stability compared to the ones with no annealing treatment. This is due to the formation of strengthened molecular packing in the annealed NDP-AB thin film, as well as the traps and defects in the semiconductor layer that can be eliminated or at least significantly reduced upon the thermal annealing treatment, resulting in the NDP-AB film hardly being doped by moisture and oxygen. To further probe the stability of NDP-AB, the as-prepared devices were measured under ambient conditions, showing an average μ_e of $1.9\times 10^{-2} \text{ cm}^2 \text{V}^{-1} \text{s}^{-1}$ (highest μ_e of $2.2\times 10^{-2} \text{ cm}^2 \text{V}^{-1} \text{s}^{-1}$), which are lower than those measured under vacuum. This suggests that during the monitoring of the charge transport mobilities, the devices can be doped by atmospheric moisture and oxygen.

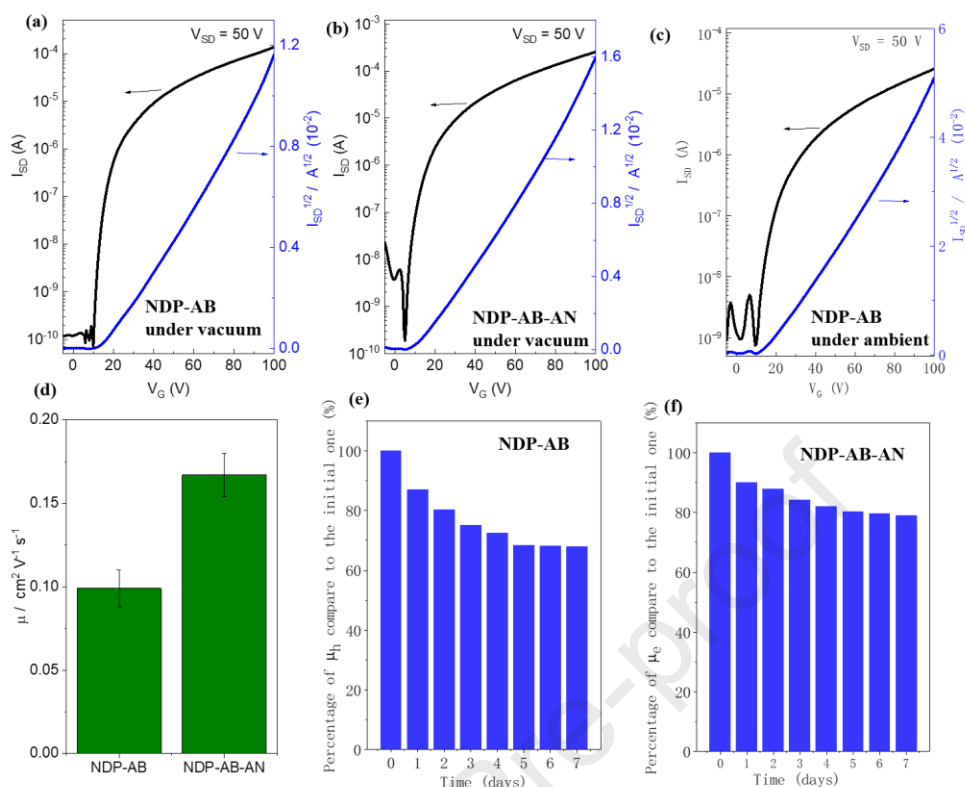


Figure 4. Transfer characteristics of the OFET devices based on NDP-AB measured under vacuum (a), NDP-AB-AN (AN: after thermal annealing at 120 °C) measured under vacuum (b) and NDP-AB measured under ambient conditions (c). (d) The calculated electron mobilities of the NDP-AB-based device with and without the thermal annealing treatment. The error bars show the variation of the mobilities from 8 different devices. (e,f) Stabilities of NDP-AB-based (e) and NDP-AB-AN-based (f) devices after the exposure to the ambient conditions.

3. Conclusions

In summary, a novel chromophore with strong electron-deficient properties, namely NDP-AB, is designed, synthesized, and characterized for OFET applications. NDP-AB exhibits a large conjugation system with highly planar core as evidenced by our DFT calculations, which is beneficial for the charge transport within the single molecules. Interestingly, the absorption in solution exhibits a 111 nm blue-shift from to that in thin film, accompanied by a clear emission quenching. These observations indicate that the NDP-AB film has a strong H-aggregation (good π - π overlap). Moreover, our XRD and AFM analyses demonstrate that the NDP-AB thin film features close π - π stacking with a small d-spacing of around 0.378 nm, which is beneficial for efficient electron transport between adjacent molecules. The electrochemical studies confirm that NDP-

AB possesses a low LUMO level, which is favorable for the electron injection from the electrode into the semiconductor layer of the n-type OFETs. The NDP-AB-based OFETs show a clear n-type behavior with a maximum electron mobility of $0.18 \text{ cm}^2 \text{ V}^{-1} \text{ s}^{-1}$. This work provides a simple and effective strategy to design a novel and strong electron-deficient chromophore, which is an attractive building block for the fabrication of high-performance n-type semiconductor materials. More importantly, NDP-AB molecules could be used as dyes, colorants, and comonomer electron-withdrawing units for photovoltaics and/or phototransistors benefiting from the enhanced light absorption in the visible range.

Conflicts of interest

The authors declare no competing financial interest.

Acknowledgements

H.Z. acknowledges the support from Young Taishan Scholars under Grant No. 201909120 and the Natural Science Foundation of China under Grant No. 21805151. M.L. thanks the Finnish Cultural Foundation (No. 00220107) for funding. P.V. acknowledges the financial support of Jane and Aatos Erkkö foundation (SOL-TECH project). This work is part of the Academy of Finland Flagship Programme, Photonics Research and Innovation (PREIN), Decision No. 320165.

References

- [1] Lakshminarayana A N, Ong A, Chi C Y. Modification of acenes for n-channel OFET materials. *Journal of Materials Chemistry C* 2022;28:10161-10440.
- [2] Someya T, Bao Z, Malliaras, G G. The rise of plastic bioelectronics. *Nature* 2016;540:379-385.
- [3] Bao Z, Chen X. Flexible and stretchable devices. *Adv Mater* 2016;28:4177-4179.
- [4] Han S, Peng H, Sun Q, Venkatesh S, Chung K-S, Chuen L-S, et al. An overview of the development of flexible sensors. *Adv Mater* 2017;29:1700375.
- [5] Zheng Y, Zhang S, Tok J, Bao Z. Molecular Design of Stretchable Polymer Semiconductors: Current Progress and Future Directions. *J Am Chem Soc* 2022.

- [6] He Q Y, Liu Y, Tan C L, Zhai W, Nam G H, Zhang H. Quest for p-Type Two-Dimensional Semiconductors. *ACS Nano* 2019;13:11:12294-12300.
- [7] Robertson J, Zhang Z F. Doping limits in p-type oxide semiconductors. *MRS Bulletin* 2021;46:1037-1043.
- [8] Ahmed S, Sinha, S K. Studies on nanomaterial-based p-type semiconductor gas sensors. *Environ Sci Pollut Res* 2022;98:11356-022-21218-6.
- [9] Asoh T, Kawabata K, Takimiya K. Carbonyl-Terminated Quinoidal Oligothiophenes as p-Type Organic Semiconductors. *Materials* 2020;13:3020.
- [10] Alsufyani M, Hallani R, Wang S H, Xiao M F, Ji X D, Paulsen B, et al. The Effect of Aromatic Ring Size in Electron Deficient Semiconducting Polymers for n-type Organic Thermoelectrics. *Journal of Materials Chemistry C* 2020.
- [11] Chen X N, Feng L N, Yu P L, Liu C, Lan J L, Lin Y H, et al. Flexible Thermoelectric Films Based on Bi₂Te₃ Nanosheets and Carbon Nanotube Network with High n-Type Performance. *ACS Applied Materials & Interfaces* 2021;13:4:5451-5459.
- [12] Huang F M, Lu D Y, Ji Y B, Gao C F, Wang X, Li W W, et al. Electron Injection Improvement of n-Type Organic Field-Effect Transistors With Indium Contact Interlayer. *IEEE Transactions on Electron Devices* 2021;68:2440-2446.
- [13] Yao B, Zhou Y, Ye X C, Wang R, Zhang J, Wan X H. A Star-Shaped Molecule with Low-Lying Lowest Unoccupied Molecular Orbital Level, n-Type Panchromatic Electrochromism, and Long-Term Stability. *Organic Letters* 2017;19:8:1990-1993.

- [14] Wang M, Li Y, Tong H, Cheng Y X, Wang L X, Jing X B, et al. Hexaazatriphenylene Derivatives with Tunable Lowest Unoccupied Molecular Orbital Levels. *Organic Letters* 2011;13:16:4378-4381.
- [15] Djurovich P I, Mayo E I, Forrest S R, Thompson M E. Measurement of the lowest unoccupied molecular orbital energies of molecular organic semiconductors. *Organic Electronics* 2009;10:515-520.
- [16] Sen T K, Mukherjee A, Modak A, Dr. Pradip Kr. Ghorai; Kratzert D, Granitzka M, et al. Phenalenyl-Based Molecules: Tuning the Lowest Unoccupied Molecular Orbital to Design a Catalyst. *Chemistry-A European Journal* 2011;18:1:54-58.
- [17] Takahiro K, Daisuke K, Jun-ichi N, Shizuo T, Yoshiro Y. Dithienylbenzobis (thiadiazole) based organic semiconductors with low LUMO levels and narrow energy gaps. *Chemical Communications* 2010;46:19:3265.
- [18] Grenz D C, Schmidt M, Kratzert D, Esser B. Dibenzo[*a,e*]pentalenes with Low-Lying LUMO Energy Levels as Potential n-Type Materials. *The Journal of Organic Chemistry* 2018;83:2:656-663.
- [19] Lee M, Kim D, Lee Y K, Koo H, Lee K T, Chung I. Indene-C60 Bisadduct Electron Transporting Material with the High LUMO Level Enhances Open-Circuit Voltage and Efficiency of Tin-Based Perovskite Solar Cells. *ACS Applied Energy Materials* 2020;3:6:5581-5588.
- [20] Zhang S, Liu J, Han Y C, Wang L X. Polymer Electron Acceptors Based on Iso-Naphthalene Diimide Unit with High LUMO Levels. *Macromolecular Chemistry and Physics* 2017;218:6:1600606.

- [21] Sun W P, Adachi Y, Ohshita J. Synthesis of thiazole-condensed germoles with enhanced electron-deficient properties. *Dyes and Pigments* 2022;203:110333.
- [22] Matsuo K, Toda N, Aratani N, Yamada H. Synthesis and Properties of the Doubly Oxonium-Embedded Picones as Electron-Deficient Polycyclic Aromatic Hydrocarbons. *Organic Letters* 2021;23:10:3986-3990.
- [23] Fang M J, Tsao C W, Hsu Y J. Semiconductor Nanoheterostructures for Photoconversion Applications. *Journal of Physics D: Applied Physics* 2020;53:143001.
- [24] Wang L Z, Zhao J H, Liu H M, Huang J. Design, modification and application of semiconductor photocatalysts. *Journal of the Taiwan Institute of Chemical Engineers* 2018;93:590-602.
- [25] Zhang Y X, Guo L D, Zhu X W, Sun X N. The Application of Organic Semiconductor Materials in Spintronics. *Frontiers in Chemistry* 2020;8:589207.
- [26] Zhang G B, Li P, Tang L X, Ma J X, Wang X H, Lu H B, et al. A bis (2-oxoindolin-3-ylidene)-benzodifuran-dione containing copolymer for high-mobility ambipolar transistors. *Chemical Communications* 2014;50:3180-3183.
- [27] Wang R, Qiao J H, He B Z, Tang X S, Wu F, Zhu L N. Electron extraction layer based on diketopyrrolopyrrole/isoindigo to improve the efficiency of inverted perovskite solar cells. *J. Mater. Chem. C* 2018;6:8429-8434.
- [28] Yamagata T, Kaneko T. The reaction of an amino-functionalized DPP with acrolein. *Tetrahedron Letters* 2022;100:153853.

- [29] Brown S J, Schlitz R A, Chabinye M L, Schuller J A. Morphology-dependent optical anisotropies in the n-type polymer P(NDI2OD-T2). *Physical Review B* 2016;94:165105.
- [30] Klimovich I, Zhilenkov A, Kuznetsova L, Frolova L, Yamilova O, Troyanov S, Lyssenko K, Troshin P. Novel functionalized indigo derivatives for organic electronics. *Dyes and Pigments* 2021;186:108966.
- [31] Klimovich I, Leshanskaya L, Troyanov S, Anokhin D, Novikov D, Piryazev A, et al. Design of indigo derivatives as environment-friendly organic semiconductors for sustainable organic electronics. *Journal of materials chemistry C* 2014;2:7621-7631.
- [32] Ngai J, Leung L, So S, Lee H. Organic soluble indigoids derived from 3-hydroxybenzaldehyde for N-type organic field-effect transistor (OFET) applications. *Organic Electronics* 2016;32:258-266.
- [33] Zhang H C, Neudörfla J M, Tieke B. 1,6-Naphthodione-based monomers and polymers. *Polymer chemistry* 2014;5:3754-3757.
- [34] Zhang H C, Yang K, Chen Y M, Bhatta R, Tsige M, et al. Polymers Based on Benzodipyrrolidone and Naphthodipyrrolidone with Latent Hydrogen-Bonding on the Main Chain. *Macromolecular Chemistry & Physics* 2017;218:1600617.
- [35] Deng Z F, Hao X L, Zhang P F, Li L Q, Yuan X Q, Ai T T, et al. Donor-acceptor-donor molecules based on diketopyrrolopyrrole, benzodipyrrolidone and naphthodipyrrolidone: Organic crystal field-effect transistors. *Dyes and Pigments* 2019;162:883–887.

- [36] Zhang H C, Zhang S, Mao Y F, Liu K W, Chen Y M, Jiang Z, et al. Naphthodipyrrolidone (NDP) based conjugated polymers with high electron mobility and ambipolar transport properties. *Polymer Chemistry* 2017;8:3255–3260.
- [37] Sheng W, Zheng Y Q, Wu Q H, Chen K K, Li M, Jiao L J, Hao E, Wang J Y and Pei J. Synthesis, characterization, and tunable semiconducting properties of aza-BODIPY derived polycyclic aromatic dyes. *Science China Chemistry* 2020;63:1240–1245.
- [38] Zhao Q Q, Yu X H, Liu J G, Xie Z Y, Han Y C. Increasing H-aggregation of p-DTS(FBTTh₂)₂ to improve photovoltaic efficiency by solvent vapor annealing. *Organic Electronics* 2016;37:6-13.
- [39] Li S, Fu L Y, Xiao X X, Geng H, Liao Q, Liao Y. Regulation of Thermally Activated Delayed Fluorescence to Room-Temperature Phosphorescent Emission Channels by Controlling the Excited-States Dynamics via J-and H-Aggregation. *Angewandte Chemie International Edition* 2021;60:18059-18064.
- [40] Zhang H C, Li R, Deng Z F, Cui S W, Wang Y H, Zheng M, Yang W J. π -Conjugated oligomers based on aminobenzodifuranone and diketopyrrolopyrrole. *Dyes and Pigments* 2020;181:108552.
- [41] Yao J J, Yu C M, Liu Z T, Luo H W, Yang Y, Zhang G X, Zhang D Q. Significant Improvement of Semiconducting Performance of the Diketopyrrolopyrrole-Quaterthiophene Conjugated Polymer through Side-Chain Engineering via Hydrogen-Bonding. *Journal of the American Chemical Society* 2016;138:1:173–185.
- [42] Coropceanu V, Cornil J, Filho D, Olivier Y, Silbey R and Brédas J. Charge Transport in Organic Semiconductors. *Chemical Reviews* 2007;107:4:926–952.

- [43] Tokoro Y, Nagai A, Chujo Y. Nanoparticles via H-aggregation of amphiphilic BODIPY dyes. *Tetrahedron Letters* 2010;51:3451-3454.
- [44] Nüesch F, Grätzel M. H-aggregation and correlated absorption and emission of a merocyanine dye in solution, at the surface and in the solid state. A link between crystal structure and photophysical properties. *Chemical Physics* 1995;193:1-17.
- [45] Liu F B, Liu J and Wang L X. Effect of fluorine substitution in organoboron electron acceptors for photovoltaic application. *Organic Chemistry Frontiers* 2019;6:1996-2003.
- [46] Sosorev A, Trukhanov V, Maslennikov D, Borshchev O, Polyakov R, Skorotetcky M, Surin N, Kazantsev M, et al. Fluorinated Thiophene-Phenylene Co-Oligomers for Optoelectronic Devices. *ACS Applied Materials & Interfaces* 2020;12:8:9507-9519.
- [47] Liu Q, Kumagai S, Manzhos S, Chen Y Q, Angunawela I, Nahid M, et al. Synergistic Use of Pyridine and Selenophene in a Diketopyrrolopyrrole-Based Conjugated Polymer Enhances the Electron Mobility in Organic Transistors. *Advanced Functional Materials* 2020;2000489.
- [48] Qiu G G, Jiang Z Y, Ni Z J, Wang H L, Dong H L, Zhang J Q, et al. Asymmetric thiophene/pyridine flanked diketopyrrolopyrrole polymers for high performance polymer ambipolar field-effect transistors and solar cells. *Journal of Materials Chemistry C* 2017;5:566-572.

- [49] Xue S, Yao L, Liu S, Shen F, Li W, Zheng H, et al. Simultaneous enhancement of the carrier mobility and luminous efficiency through thermal annealing a molecular glass material and device. *Journal Materials Chemistry* 2012;22:21502-21506.
- [50] Xue S, Fei T, Yao L, Sheng F, Zhang M, Liu X, et al. Low-temperature annealing to enhance efficiency in organic small-molecule solution-processable OLEDs. *Semiconductor Science and Technology* 2011; 26:055016.
- [51] Silva B P, Lemes R P G, Zanatta G, Rodrigues d S, Regina C, Lima-Neto P D. Solid state properties of hydroxyurea: Optical absorption measurement and DFT calculations. *Journal of Applied Physics* 2019;125:13:134901.
- [52] Guo Z L, Wang R J, Liang Y F, Liu G, Pu S Z. Synthesis and properties of photochromic hybrid diarylethenes bearing benzothiophene and pyrrole moieties. *Tetrahedron Letters* 2021;68:152910.
- [53] Kim J H, Matsuoka M, Fukunishi K. Synthesis and solid state absorption spectra of some aminonaphthoquinone dyes. *Dyes and Pigments* 1996;31:263-272.
- [54] Nicoli F, Roos M K, Hemmig E A, Di A M, de Vivie-Riedle R, Liedl T. Proximity-Induced H-Aggregation of Cyanine Dyes on DNA-Duplexes. *The Journal of Physical Chemistry A* 2016;120:50:9941-9947.
- [55] Yuan J, Wang S, Ji Y, Chen R F, Zhu Q, Wang Y R, et al. Invoking ultralong room temperature phosphorescence of purely organic compounds through H-aggregation engineering. *Materials Horizons* 2019;6:1259-1264.

- [56] Hong J X, Xia Q F, Zhou E B, Feng G Q. NIR fluorescent probe based on a modified rhodol-dye with good water solubility and large Stokes shift for monitoring CO in living systems. *Talanta* 2020;215:120914.
- [57] Zhao Y N, Ding J, Han X, Geng T, Zhou X W, Hu C, et al. Tuning the optical properties of N-aryl benzothiadiazole via Cu(ii)-catalyzed intramolecular C-H amination: the impact of the molecular structure on aggregation and solid state luminescence. *Organic Chemistry Frontiers* 2020;7:3853-3861.
- [58] Li D P, Wang H L, Kan J L, Lu W J, Chen Y L, Jiang J Z. Materials design for high-performance air-stable ambipolar organic thin film transistors. *Organic Electronics* 2013;14:2582-2589.
- [59] Han G C, Shen X X, Duan R H, Geng H, Yi Y P. Revealing the influence of the solvent evaporation rate and thermal annealing on the molecular packing and charge transport of DPP(TBFu)₂. *Journal of Materials Chemistry C* 2016;4:4654-4661.
- [60] Song H G, Kim Y, Park So-Min, An T K, Kwon Soon-Ki, Park C E, et al. Synthesis, characterization, and transistor applications of new linear small molecules: Naphthyl-ethynyl-anthracene-based small molecules containing different alkyl end group. *Dyes and Pigments* 2016;131:349-355.
- [61] Jiang S, Zhang R, Zhang X B, Zhang Y, Dong Z C. Bicomponent supramolecular self-assemblies studied with tip-enhanced Raman spectroscopy. *Journal of Raman Spectroscopy* 2021;52:366-374.

- [62] Wu B Q, Zhang Y, Tian S Z, Oh J, Yang M Q, Pan L H, et al. Non-Fused Polymerized Small Molecular Acceptors for Efficient All-Polymer Solar Cells. *Solar RRL* 2022;6:2101034.
- [63] Glowacki E D, Coskun H C, B-Forsythe M A, Mibjiwuys U, Leonat L, et al. Hydrogen-bonded diketopyrrolopyrrole (DPP) pigments as organic semiconductors. *Organic Electronics* 2014;15:3521-3528.
- [64] Suna Y, Nishida J, Fujisaki Y, Yamashita Y. Ambipolar behavior of hydrogen-bonded diketopyrrolopyrrole-thiophene co-oligomers formed from their soluble precursors. *Organic Letters* 2012;14:3356-3359.
- [65] Zhang H, Deng R, Wang J, Li X, Chen Y-M, Liu K, et al. Crystalline Organic Pigment-Based Field-Effect Transistors. *ACS Applied Interfaces* 2017;9:21891-21899.
- [66] Cui S, Liang D, Liu M, Vivo P, Zheng M, Zhuang T, et al. *Advanced Electronic Materials* 2022;2200019.
- [67] Chapran M, Angioni E, Findlay N, Breig B, Cherpak V, et al. An ambipolar BODIPY derivative for a white exciplex OLED and cholesteric liquid crystal laser toward multifunctional devices. *ACS Applied Interfaces* 2017;9:4750-4757.

Highlight:

1. Naphthodipyrrolopyrrole-based dimeric aza-boron dipyrromethene (aza-BODIPY) chromophore, namely NDP-AB, is for the first time designed and synthesized.
2. NDP-AB exhibits not only strong electron-deficient ability with ultra-low LUMO energy level of -4.25 eV, but also large conjugation system.
3. NDP-AB features strong H-aggregation.
4. NDP-AB-based OFETs demonstrate n-type properties with an average electron mobility of $0.16 \text{ cm}^2 \text{ V}^{-1} \text{ s}^{-1}$.
5. NDP-AB is a promising electron-deficient building block for the fabrication of high-performance n-type semiconductors.

Conflict of Interest

The authors declare no conflict of interest.

Journal Pre-proof